Published online 29 July 2017 *Nucleic Acids Research, 2017, Vol. 45, No. 17* ***10259–10269***
doi: 10.1093/nar/gkx669

An RNA-targeted therapy for dystrophic epidermolysis bullosa

Patricia Peking[1], Ulrich Koller[1], Blanca Duarte[2], Rodolfo Murillas[2], Susanne Wolf[3], Tobias Maetzig[3], Michael Rothe[3], Thomas Kocher[1], Marta García[2], Gabriele Brachtl[4], Axel Schambach[3,5], Fernando Larcher[2,6], Julia Reichelt[1], Johann W. Bauer[7] and Eva M. Murauer[1,*]

[1]EB House Austria, Research Program for Molecular Therapy of Genodermatoses, Department of Dermatology, University Hospital of the Paracelsus Medical University Salzburg, Austria, [2]Epithelial Biomedicine Division, CIEMAT-CIBERER, Department of Bioengineering, UC3M, Madrid, Spain, [3]Institute of Experimental Hematology, Hannover Medical School, Hannover, Germany, [4]Institute for Experimental and Clinical Cell Therapy, Core Facility for Flow Cytometry, SCI-TRECS, Paracelsus Medical University, Salzburg, Austria, [5]Division of Hematology/Oncology, Boston Children's Hospital, Harvard Medical School, Boston, MA, USA, [6]Instituto de Investigación Sanitaria de la Fundación Jiménez Díaz, Madrid, Spain and [7]Department of Dermatology, University Hospital of the Paracelsus Medical University, Salzburg, Austria

Received May 11, 2017; Revised July 11, 2017; Editorial Decision July 19, 2017; Accepted July 20, 2017

ABSTRACT

Functional impairment or complete loss of type VII collagen, caused by mutations within *COL7A1*, lead to the severe recessive form of the skin blistering disease dystrophic epidermolysis bullosa (RDEB). Here, we successfully demonstrate RNA *trans*-splicing as an auspicious repair option for mutations located in a wide range of exons by fully converting an RDEB phenotype in an *ex vivo* pre-clinical mouse model based on xenotransplantation. Via a self-inactivating (SIN) lentiviral vector a 3′ RNA *trans*-splicing molecule, capable of replacing *COL7A1* exons 65–118, was delivered into type VII collagen deficient patient keratinocytes, carrying a homozygous mutation in exon 80 (c.6527insC). Following vector integration, protein analysis of an isolated corrected single cell clone showed secretion of the corrected type VII collagen at similar levels compared to normal keratinocytes. To confirm full phenotypic and long-term correction *in vivo*, patches of skin equivalents expanded from the corrected cell clone were grafted onto immunodeficient mice. Immunolabelling of 12 weeks old skin specimens showed strong expression of human type VII collagen restricted to the basement membrane zone. We demonstrate that the RNA *trans*-splicing technology combined with a SIN lentiviral vector is suitable for an *ex vivo* molecular therapy approach and thus adaptable for clinical application.

INTRODUCTION

The severe phenotype of the skin blistering disease dystrophic epidermolysis bullosa (DEB) results from malfunctioning or absence of type VII collagen protein, induced by mutations in *COL7A1* (1). Type VII collagen is a linker protein of 290 kDa in size, which assembles to anchoring fibrils within the basement membrane zone (BMZ) of the skin when secreted from epidermal keratinocytes and dermal fibroblasts. In healthy skin, cross-linking anchoring fibrils ensure the attachment of the epidermis to the underlying dermis through interaction with other BMZ and matrix components. Dysfunction of anchoring fibrils induces skin blistering and recurrent wounding in DEB patients (2,3). Severe generalized recessive DEB (RDEB) is characterized by total absence of type VII collagen protein and consequent deficiency of anchoring fibrils. These patients suffer from strong pain, extensive skin blistering accompanied by chronic infections and mutilating scarring. Moreover, individuals with RDEB have a high risk of developing aggressive metastasizing squamous cell carcinomas in skin areas bearing chronic ulcers, which can lead to premature death in the third to fourth decade of life (4). Other than symptomatic treatments there is no effective therapy available. Therefore, the development of a causative therapy for RDEB is urgently needed.

Cutaneous genes, amongst them *COL7A1* with a huge size of ∼9 kb when transcribed, contain highly repetitive sequences, which might complicate inclusion in a cDNA replacement therapy due to limited vector packaging capacities as well as low viral titers, impeding delivery of large,

*To whom correspondence should be addressed. Tel: +43 5 7255 80930; Fax: +43 5 7255 82497; Email: e.murauer@salk.at

repetitive sequences into cells (5,6). It has turned out that the spliceosome mediated RNA *trans*-splicing technology, SMaRT, offers a promising option to correct monogenetic disease phenotypes (7,8). SMaRT uses naturally occurring splicing mechanisms within the cell to replace a disease-causing mutated region within a targeted pre-mRNA by its wild-type version, and has previously been described for inherited diseases such as spinal muscular atrophy (9), Huntington disease (10), or Alzheimer's disease (11). The splicing reaction is induced by an RNA *trans*-splicing molecule (RTM), which contains a binding domain (BD) specifically hybridizing to a short sequence of the target pre-mRNA, splicing elements for efficient splicing, and the wild-type coding sequence to be *trans*-spliced into the pre-mRNA. The RTM can be designed to exchange either 5′, 3′ or internal pre-mRNA parts and is therefore suitable for the repair of any known mutation within a given transcript (7,8,12). Reduced transgene sizes compared to a vector carrying full-length cDNA leads to higher particle output from vector producer cells including lower error rates during reverse transcription, resulting in increased infectivity and gene transfer rates. Further, RNA *trans*-splicing offers other important advantages such as avoidance of ectopic expression of a transgene, in favor of maintenance of endogenous regulation of the repaired mRNA and the possibility to correct dominant negative mutations, allowing the treatment of recessively and dominantly inherited diseases (13). Previously, we successfully corrected an RDEB phenotype *in vitro* by the application of a 3′ RTM (RTM-S6) expressed in a retroviral vector (14). In the present study, we moved forward towards a clinical application by improving the specificity and safety of the previously designed RTM-S6 (now termed RTM-S6m) and confirming its functionality in an *ex vivo* therapy approach using a xenograft mouse model. The RTM-S6m replaces mutations over a 3,300 bp sequence spanning from exon 65 to exon 118 of the *COL7A1* mRNA, encompassing nearly 40% of all DEB causing mutations (15,16).

Focusing on the development of a safe pre-clinical approach, we have chosen a lentiviral, self-inactivating (SIN) vector system for the delivery of RTM-S6m (LV-RTM-S6m) into RDEB keratinocytes.

To achieve efficient type VII collagen correction, we isolated keratinocyte clones of transduced cell pools, and one (C47) was selected for all subsequent experiments to analyze the functional correction of type VII collagen expression *in vitro* and in human skin grafts.We demonstrate here the first proof that 3′ *trans*-splicing is capable of long-term correction of the RDEB phenotype in an *ex vivo* RNA therapy approach.

MATERIALS AND METHODS

Cloning of RTM-S6m into a self- inactivating (SIN) lentiviral expression vector (LV-RTM-S6m)

The bidirectional lentiviral vector was constructed based on pLBid.nC.GFP.SF.mCherry.pre* (17) by first introducing a multiple cloning site 5′ of the SV40 pA, and simultaneously inversing the orientation of the internal mCMV.SFFV bidirectional promoter cassette with regard to the vector configuration, so that mCMV drives eGFP expression in sense, and SFFV drives expression of a potential antisense transcript within the multiple cloning site. In the next step, eGFP was exchanged by a GFP-2A-Puro transgene cassette. This plasmid served as acceptor for RTM via XbaI/HindIII digestion yielding LV-RTM-S6m and LV-RTM-woBD, respectively.

Cell culture, lentiviral transduction and isolation of single clonal cells

Immortalized RDEB keratinocytes, carrying a homozygous mutation in exon 80 (c.6527insC), were prepared as previously described (18) and cultivated in keratinocyte medium containing DMEM:Ham's F-12:fetal calf serum (6:3:1) (HyClone/Perbio Science, Brezons, France), supplemented with 4 mM glutamine and 1 mM sodium-pyruvate (Sigma-Aldrich, Taufkirchen, Germany). In order to transduce RDEB keratinocytes lentiviral particles, including 1.8 μg NovB2 to increase the viral titer, were harvested from culture medium 48 h post-transfection of 293T cells and added to RDEB keratinocytes in the presence of polybrene (10 μg/ml medium) at 37°C and 5% CO_2. Transduced cells were then selected in the presence of 1 μg puromycin/ml medium for 7 days. Single GFP-expressing cells of the LV-RTM-S6m transduced RDEB keratinocytes population were isolated by fluorescence activated cell sorting (FACS), using the cell sorter FACS AriaIII (BD Bioscience, Franklin Lakes, NJ, USA) to obtain a homogenous cell population, expressing the *trans*-splicing repaired *COL7A1* transcripts. 480 GFP positive single cells were sorted and cultivated in 96-well plates in DMEM:Ham's F-12 (3:1) (19), amongst them were about 160 cells viable after the sorting process. For further analysis 33 selected clones, showing rapid growth were included.

Immunofluorescence staining of cultivated cells

RDEB keratinocytes were cultivated in Lab-Tek Chamber slides (Sigma-Aldrich), fixed in 4% formaldehyde (Sigma-Aldrich) for 30 min and blocked in 1% bovine serum albumin (BSA), 0.5% Triton X-100 (Sigma Aldrich) in PBS (Invitrogen, Paisley, UK) for 45 min. As primary antibody, a polyclonal anti-type VII collagen antibody (Calbiochem, San Diego, CA, USA) was used and diluted 1:100 in PBS. After incubation for 1 h at room temperature, cells were incubated with the secondary antibody anti-rabbit AF594 (Invitrogen) for an additional hour in a dilution of 1:400 in PBS in the dark. DAPI (Sigma-Aldrich) staining of the nuclei was performed in a dilution of 1:2000 for 10 min. After mounting (Dako, Vienna, Austria), the sections were analyzed under an inverted confocal laser scanning microscope (LSM700, Carl Zeiss). Images were converted to tiff files with the ZEN Black 2011 (Carl Zeiss) software.

PCR analysis of genomic DNA

Genomic DNA of transduced keratinocytes was isolated using the DNeasy Blood and Tissue Kit (Qiagen, Hilden, Germany) according to the manufacturer's protocol. For detection of full-length LV-RTM-S6m, PCR analysis using a polyA signal specific forward

primer (5′CCTCCCCCTGAACCTGAAACATAAAATG AATGC3′), a *COL7A1* exon 65 specific reverse primer (5′GATTCAGGCGCCTCTGGGAGAGAAG3′) as well as the Long Range dNTPack (Roche, Vienna, Austria) was performed according to the manufacturer's protocol. PCR products were verified by sequence analysis.

RNA isolation and cDNA synthesis

Keratinocytes were harvested at confluence of 70% and RNA was isolated using RNeasy Mini Kit (Qiagen) according to the manufacturer's protocol. 1–3 μg RNA were digested with DNaseI (Sigma-Aldrich) for 30 min at RT. cDNA synthesis was performed using the iScript™ cDNA Synthesis Kit (Bio-Rad, Munich, Germany) according to manufacturer's protocol.

sqRT-PCR analysis

For detection of *trans*-spliced *COL7A1* transcripts in LV-RTM-S6m transduced RDEB keratinocytes, an exon 61/62 specific forward primer (5′TGGGCCGAATGGTGCTG CA3′) and an exon 65 polymorphism specific reverse primer (5′CTGAATCTCCCTTTTCACCCTTACG3′), cDNA of transduced cells and GoTaq® qPCR Master Mix (Promega Madison, WI, USA) were included in the PCR. For detection of *cis*-spliced *COL7A1* mRNA expression we used the same forward primer and a reverse primer specific for *COL7A1* exon 65 (5′CTGAATCTCCTTTCTCTCCCTTC CT3′). The PCR was performed using a Bio-Rad CFX™ system under following conditions: 95°C for 2 min, and 50 cycles of 20 s at 95°C, 20 s at 67°C, and 20 s at 72°C. The correct PCR products were verified by sequence analysis. For relative quantification the $2^{\wedge\Delta c(t)}$ method was used, using four independent experiments and mean of duplicates.

Western blot analysis

Cells were grown to confluence in keratinocyte medium, then the medium was switched to serum-free CnT-Prime epithelial cell medium (CELLNTEC, Bern, Switzerland) including 50 μg/ml ascorbic acid and incubated for 48 h. The supernatant was supplemented with 7× Complete protease inhibitor (Roche) and protein was precipitated in 100% ammonium sulfate (Merck, Darmstadt, Germany) at 4°C over night. After a centrifugation step for 30 min at 3000g at 4°C the protein pellet was resuspended in an appropriate volume (50–80 μl) of 8 M urea (Merck). For extraction of the cell lysate, cells were washed with PBS, harvested and resuspended in radioimmunoprecipitation assay buffer (RIPA buffer; Santa Cruz Biotechnology, Heidelberg, Germany). All protein samples were denatured for 5 min at 95°C in 4× loading buffer (0.25 M Tris|HCl; 8% SDS; 30% glycerol; 0.02% bromphenol blue; 0.3 M β-mercaptoethanol; pH 6.8). Western blotting was performed as previously described (20). Ponceau S (Sigma-Aldrich) staining of the membrane was performed after electro-blotting. Primary antibody: pAb against the NC-1 domain of type VII collagen (LH7.2, kindly provided by Dr. Alexander Nyström from Freiburg) or polyclonal anti-type VII collagen antibody (Calbiochem) diluted 1:3000 and 1:1000, respectively, in 0.2% TBS–Tween and incubated over night at 4°C. Secondary antibody: HRP Envision+ labelled anti-rabbit antibody (Dako), diluted 1:250. Protein bands were visualized using the Immobilon Western Chemiluminescent HRP Substrate (Merck) and the ChemiDoc XRS Imager (Bio-Rad). Relative quantification analysis of type VII collagen bands was performed using the Image Lab™ 5.2.1 software (BioRad). All type VII collagen bands were normalized to the loading control α-actinin.

Adhesion assay

For *in vitro* adhesion assay 30 000 keratinocytes were seeded onto fibronectin- and type IV collagen-coated 96-well plates (BioPioneer, San Diego, CA, USA) and the assay was performed according to the manufacturer's protocol. BSA control values were substracted from the measured OD570 values, which were then referred to OD570 from polyLysin.

Southern blot analysis

To detect full-length RTM integration, genomic DNA was extracted and digested with HindIII (Roche), which flanks the RTM, resulting in a 4.4 kb DNA fragment, using an RTM specific probe. For evaluation of the VCN genomic DNA was digested with Asp718 (Roche), resulting in a 7 kb fragment, detectable using a GFP specific probe. Digested DNA was separated on a 0.8% agarose gel, transferred to a nylon membrane (Hybond XL, GE Healthcare) and either probed with the ^{32}P-radiolabeled sequence of a fragment of the RTM (Exon65- exon70- spacer) to detect specific (4.4 kb) and non-specific, rearranged integrations or probed with the ^{32}P-radiolabeled sequence of a fragment of GFP to detect the number of integration events. To detect the radiolabel signal membranes were exposed to phosphor screens and visualized using Phosphorimaging (Bio-Rad Molecular Imager FX) and they were exposed in an automatic reveal machine Curix60 (AGFA).

Mouse transplantations

Grafting of LV-RTM-S6m corrected skin equivalents was performed as previously described (21–23). For each time point and sample six mice were grafted, among them were at least two informative grafts. Skin grafts were harvested 4 and 12 weeks after transplantation for further analysis.

Histological and immunofluorescence analysis of skin cryosections

Punch biopsies were taken from harvested mouse skin and frozen at –20°C. Sections of 8 μm were generated on glass microscope slides (Star Frost, Laborchemie GmbH, Vienna, Austria) with a cryotome (MICROM HM 550, Thermo Fisher Scientific Inc., Runcorn, UK). For histological analysis sections were stained with hematoxylin (Merck) and eosin (Merck). For immunofluorescence staining sections were fixed in ice cold aceton (Merck) for 2 min and blocked in 0.5% BSA (Sigma-Aldrich) in PBS (Invitrogen) for 60 min. Primary antibodies were: pAb against the NC-1 domain of type VII collagen (LH7.2, kindly provided by Dr. Alexander Nyström from Freiburg) produced

in rabbit diluted 1:3000 in PBS for 90 min, monoclonal anti-involucrin (Santa Cruz Biotechnology, Heidelberg, Germany), 1:100 for 2 h. The secondary antibody anti-rabbit AF594 and anti-mouse AF488 (Invitrogen) were incubated for 1 h in a 1:400 dilution in PBS in the dark. DAPI (Sigma-Aldrich) staining of the nuclei (Sigma-Aldrich) was performed in dilution of 1:2000 for 10 min. After mounting, using a fluorescence aqueous mounting medium (Dako), the sections were observed under the confocal laser scanning unit (Axio Observer Z1 attached to LSM710, Zeiss) and images were converted to TIFF files with the ZEN Blue 2012 (Carl Zeiss) software.

Statistical analysis

Statistical significance was evaluated by a *t*-test (sqRT PCR) and a one-way ANOVA including a Tukey's multiple comparison test (adhesion assays) in GraphPad Prism.

Approval of animal studies

Procedures were approved by the Animal Experimentation Ethical Committee of the CIEMAT according to all external and internal bio-safety and bio-ethics guideline, and by Spanish competent authority with registered number PROEX 187/15.

RESULTS

Correction of RDEB patient keratinocytes by transduction with the RTM-S6m expressed in a lentiviral vector

The recently published RTM-S6 (14,24), containing the wild-type sequence of *COL7A1* exons 65–118, a 3′ splice site (ss) and a BD, which is 224 nt long and complementary to the endogenous *COL7A1* intron 64/exon 65 junction was optimized in terms of specificity and safety (RTM-S6m). We removed a cryptic ss located 5 nt upstream of the 3' ss in the linker sequence (AG deletion), in order to avoid cryptic splicing as recently reported (24) and possible expression of truncated proteins (Supplementary Figure S1A). Further, an in frame start codon within the BD was removed (T>C transition) to minimize the risk of direct RTM expression followed by shortened protein translation (Supplementary Figure S1B). The optimized construct was confirmed by sequence analysis (Supplementary Figure S1A and B). Introduced polymorphisms (6 silent mutations) into *COL7A1* exons 65 and 66 of the RTM-S6m allow discrimination between *cis*- and *trans*-spliced mRNA. The RTM-S6m was cloned in antisense direction into a self-inactivating lentiviral vector (SINpLbid-nC-RTM-S6m), and was termed LV-RTM-S6m. The 5′ polyA signal lowers the risk of insertional mutagenesis, thus we conceded the lower viral titer production. The fact that *trans*-splicing only occurs in cells expressing the endogenous target mRNA ensures tissue-specific transgene activity, allowing the use of a strong viral promoter instead of a weak tissue-specific *COL7A1* promoter in order to assure high level expression of LV-RTM-S6m. LV-RTM-S6m additionally expresses a GFP / puromycin cassette under the control of a minimal (mn) CMV promoter to facilitate the selection of transduced target cells (17) (Figure 1A).

Integration and subsequent expression of the LV-RTM-S6m in target cells induces *trans*-splicing-mediated replacement of the endogenous *COL7A1* pre-mRNA (Figure 1B). We further used an RTM without BD expressed in the same vector (LV-RTM-woBD) as a suitable control to point out the influence of the BD to the specificity and efficiency of the *trans*-splicing reaction. Both viral constructs (LV-RTM-S6m and LV-RTM-woBD) were stably transduced into a human RDEB keratinocyte line, carrying a homozygous mutation in exon 80 (c.6527ins C) of *COL7A1*, which leads to a 321 bp downstream stop mutation, and consequently to type VII collagen deficiency. A virtual transduction efficiency of 60% was achieved, and 98% of the transduced keratinocytes carried the vector after puromycin selection as verified by GFP expression (data not shown). Vector integration into the genome was detected by amplifying the 3.6 kb full-length RTM by PCR of genomic DNA from LV-RTM-S6m and LV-RTM-woBD transduced keratinocytes, respectively (Figure 1C). The correct sequences of the RTM-S6m were confirmed by sequence analysis (data not shown).

Verification of type VII collagen correction in LV-RTM-S6m transduced RDEB keratinocytes

By immunofluorescence staining of the transduced bulk cell population (cell pool) we could detect type VII collagen expression in about 40–50% of LV-RTM-S6m transduced RDEB keratinocytes at an intensity comparable to wild-type keratinocytes. Untransduced and LV-RTM-woBD expressing cell populations showed only a very faint staining of type VII collagen probably due to a residual expression of the mutated protein within the cytoplasm (Figure 1D).

Analysis of functional correction of type VII collagen expression in the selected single cell clone C47

33 LV-RTM-S6m corrected RDEB single cell clones were analyzed via immunofluorescent staining using a type VII collagen specific antibody. Eleven (∼33%) clones expressed an increased amount of type VII collagen in comparison to untreated patient keratinocytes, and two clones (∼6%) displayed protein expression levels similar to normal (data not shown). For further analysis, we selected the single cell clone C47, which showed type VII collagen expression at an intensity comparable to normal keratinocytes. Untransduced and LV-RTM-woBD expressing RDEB keratinocytes were negative for specific type VII collagen staining (only faint background expression was visible) (Figure 2A).

Immunoblotting of cell lysates extracted from LV-RTM-S6m corrected cells confirmed the expression of full-length 290 kDa type VII collagen in clone C47, slightly detectable in untreated and LV-RTMm-woBD treated cells. Relative quantification of type VII collagen expression levels in cell lysates revealed ∼53% protein expression compared to normal keratinocytes (100%), whereat in untransduced RDEB keratinocytes only ∼6% type VII collagen is expressed. Western Blot analysis of supernatants collected from C47 confirmed subsequent secretion of full-length type VII collagen, which was exclusively detectable in the C47 clone (Figure 2B).

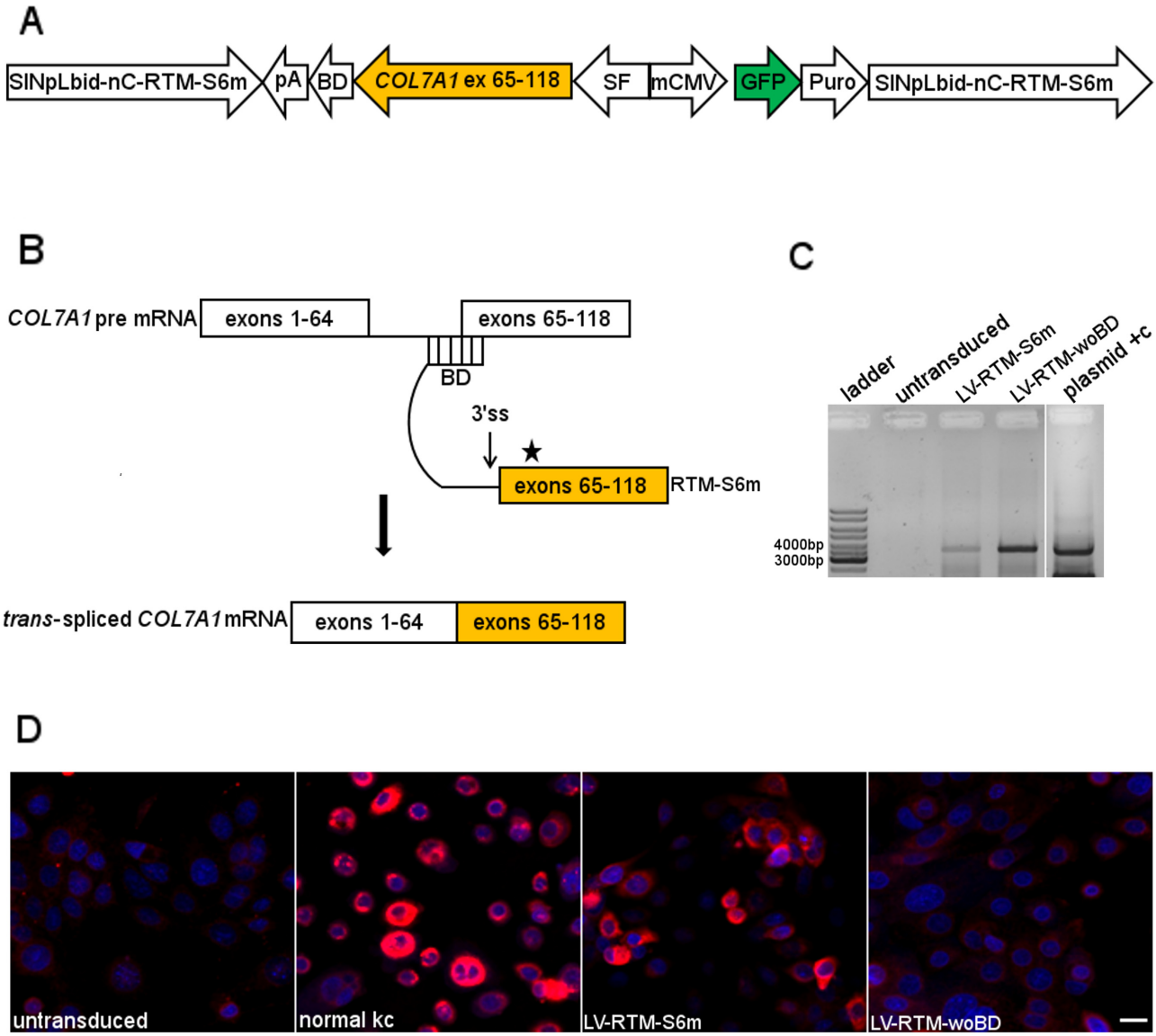

Figure 1. LV-RTM-S6m transduced RDEB patient keratinocytes showed *trans*-splicing corrected type VII collagen expression. (**A**) The bidirectional SIN lentiviral vector contained the coding sequence of *COL7A1* exons 65–118 and the 224 bp BD in antisense direction expressed by a spleen focus forming virus promoter (SF-Pro). The GFP and puromycin cassette (Puro) under the control of a mnCMV promoter was inserted in sense direction. (**B**) Stable transduction of LV-RTM-S6m into an RDEB keratinocyte cell line induced accurate *trans*-splicing into the endogenous *COL7A1* pre-mRNA, leading to the replacement of endogenous *COL7A1* exons 65–118 by a wild-type copy provided by the RTM. Asterisk = silent mutations. (**C**) PCR analysis on genomic DNA of LV-RTM-S6m and LV-RTMm-woBD transduced RDEB keratinocytes showed full-length genomic RTM integration (3.6 kb). Positive control: LV-RTM-S6m plasmid. (**D**) Immunofluoresence staining showed a specific signal indicating type VII collagen expression (red) in LV-RTM-S6m transduced RDEB keratinocytes, similar to healthy wild-type keratinocytes (normal kc) and hardly visible in negative controls (untransduced and LV-RTMm-woBD). Cell nuclei: 4′,6-diamidin-2-phenylindol (DAPI, blue). Scale bar (SB) = 20 μm.

We further investigated the functionality of *trans*-splicing corrected type VII collagen expressed from the C47 cell clone using adhesion assays. Generation of functional type VII collagen is characterized by interaction of the NC-1 domain with extracellular matrix (ECM) proteins, such as collagen IV and fibronectin (25–27). The results indicated a significantly increased ability of C47 keratinocytes to attach to collagen IV and fibronectin, compared to untransduced and LV-RTMm-woBD transduced RDEB keratinocytes (Figure 3).

Analysis of accurate *trans*-splicing of *COL7A1* mRNA in the single cell clone C47

Accurate *trans*-splicing into *COL7A1* transcripts was detected via semi-quantitative real time (sqRT)-PCR on cDNA of LV-RTM-S6m transduced cell pool and in the single cell clone C47 using primers specific for the endogenous *COL7A1* exon 62/63 junction and the introduced polymorphism in exon 65/66 of LV-RTM-S6m, respectively (Figure 4A, Supplementary Figure S2A). The correct sequence of the amplified 216 bp PCR product was confirmed by sequence analysis (Figure 4B).

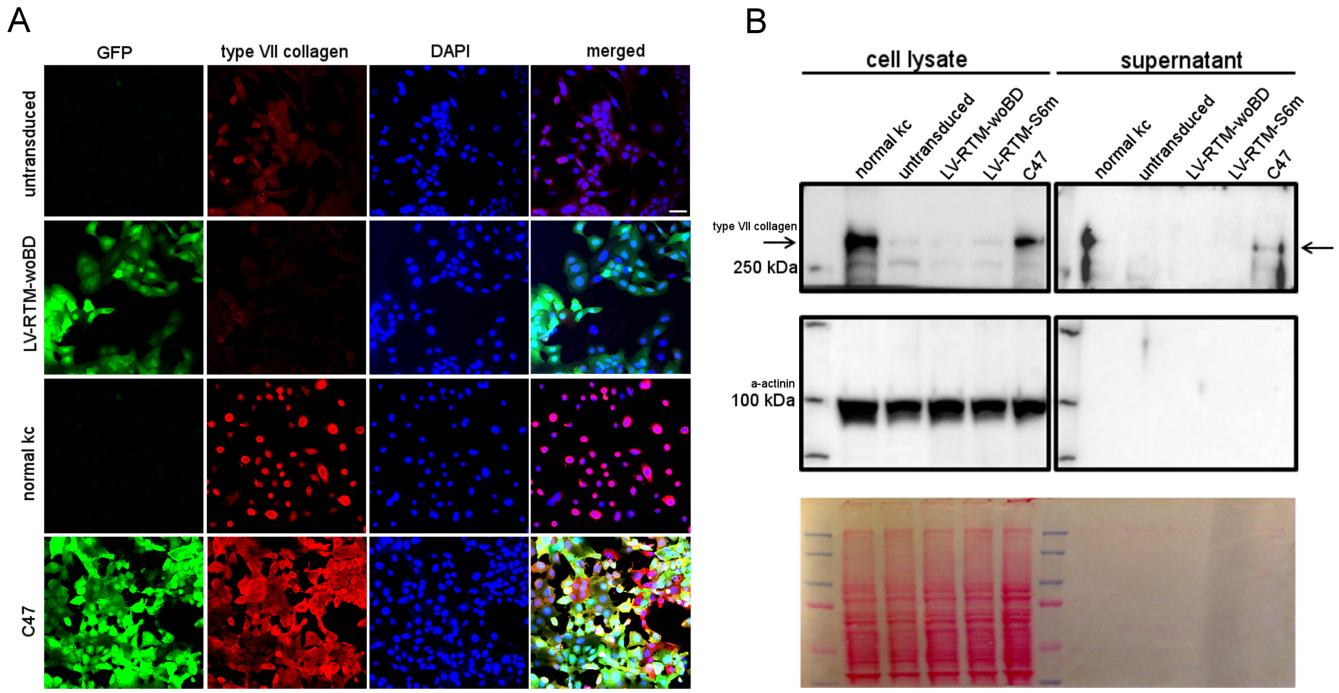

Figure 2. Single cell clone C47 showed strong type VII collagen expression. (**A**) Immunofluorescence analysis showed strong type VII collagen expression (red) in C47. Vector integration in transduced keratinocytes was confirmed by GFP expression (green). The cell nuclei were stained with DAPI (blue). SB = 50 μm. (**B**) Immunoblotting of extracted cell lysates and supernatants revealed expression as well as secretion of corrected type VII collagen in C47 (arrows), barely visible in untransduced and LV-RTMm-woBD transduced RDEB keratinocytes. Positive control: normal keratinocytes (kc). α-actinin and Ponceau staining confirmed equal loading.

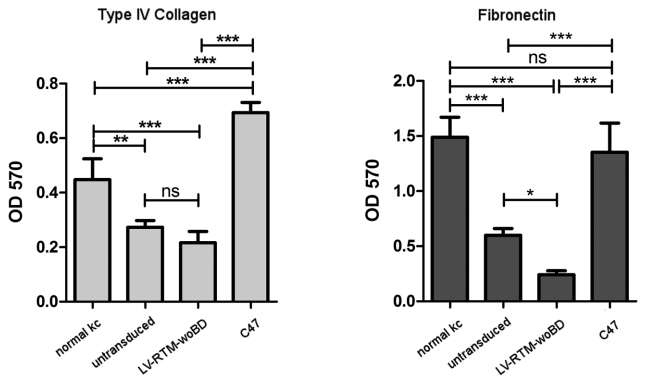

Figure 3. *Trans*-splicing corrected type VII collagen expression is functional. C47 showed an increased binding ability to the ECM proteins collagen IV and fibronectin compared to untransduced and LV-RTM-woBD transduced RDEB keratinocytes. Mean of four values for collagen IV and five values for fibronectin and error bars (SEM) including one-way ANOVA analysis with a Tukey's multiple comparison test are given. ns = not significant; **P*-value < 0.05; ***P*-value < 0.01; ****P*-value < 0.001.

Quantification of *trans*-spliced versus *cis*-spliced *COL7A1* mRNA

The ratio of *cis*-spliced mRNA compared to *trans*-spliced mRNA was determined by performing sqRT-PCR analysis using forward primers binding to endogenous *COL7A1* exon 62/63 and reverse primers binding either to the introduced polymorphism (*trans*-splicing) or to the same region without silent mutations (*cis*-splicing). Quantification analysis showed that in C47 2.113% of total transcribed mRNA were corrected by *trans*-splicing (Figure 4C, Supplementary Figure S2B).

Analysis of vector integration in the LV-RTM-S6m corrected single clone C47

Full-length RTM integration in LV-RTM-S6m, LV-RTM-woBD transduced cell pools and single cell clone C47 was indicated by Southern blot analysis. Genomic DNA was digested with HindIII, which flanks the RTM, and the predicted band at 4.4 kb, using a 327 bp probe, spanning the sequence from *COL7A1* exon 70 to parts of the spacer sequence of LV-RTM-S6m was detected (Figure 5A and B). Shorter fragments arising from rearranged proviruses were not detectable (Figure 5B).

We determined the vector copy number (VCN) in several of the screened cell clones in order to select one clone, showing the highest level of type VII collagen expression upon *trans*-splicing correction together with the lowest number of integrated proviral copies into the cell's genome. The VCN was determined by PCR analysis on genomic DNA of LV-RTM-S6m transduced keratinocytes, and single cell clones, which gave an average of 1.34 ± 0.06 for the mixed LV-RTM-S6m transduced cell population and 1.25 ± 0.02 for the C47 derived cell population (Supplementary Figure S3A). Other cell clones showed up to 2.25 ± 0.14 integrated copies (data not shown). In order to confirm the VCN, we performed Southern Blot analysis using the restriction enzyme Asp718 and a probe hybridizing to the

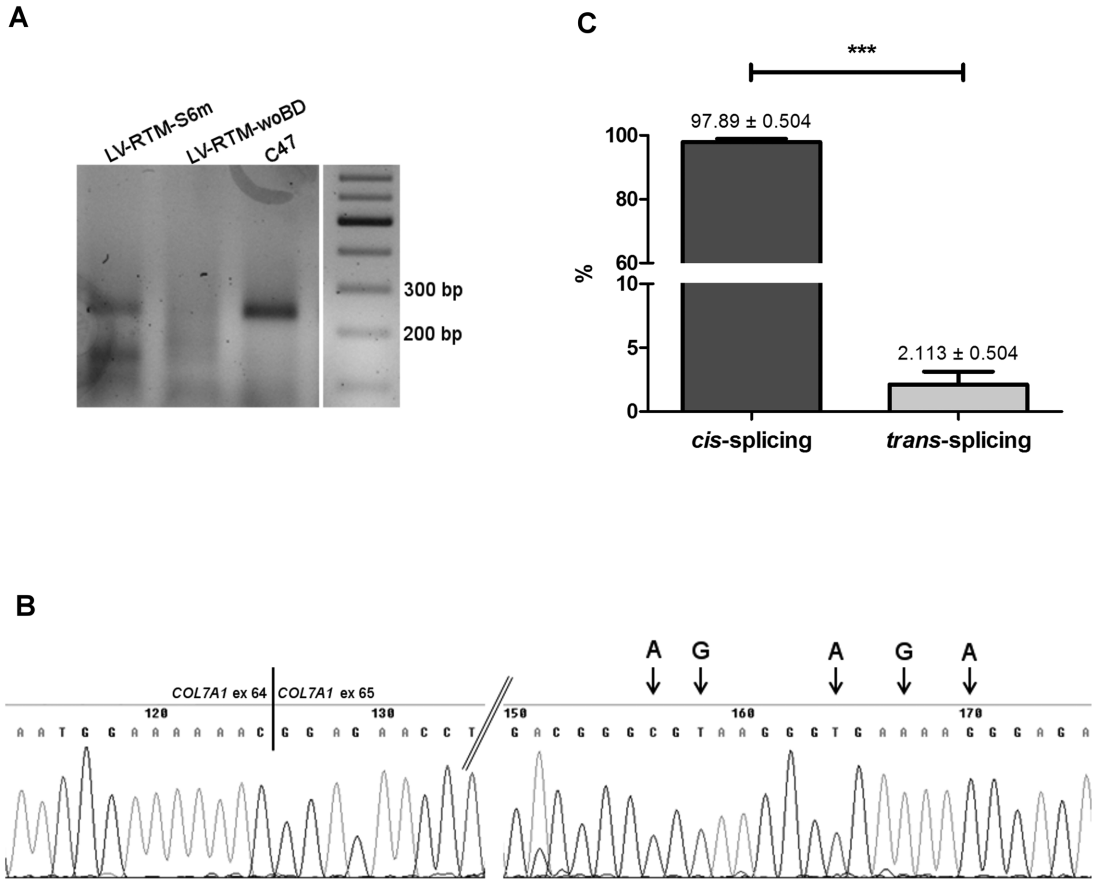

Figure 4. Analysis of the *trans*-spliced *COL7A1* mRNA in the LV-RTM-S6m corrected RDEB single cell clone C47. (**A**) Via sqRT-PCR using primers specifically hybridizing to endogenous *COL7A1* exon 62/63 and the introduced silent mutation in exon 65 on the RTM, we detected a product of 216 bp, corresponding to the *trans*-spliced *COL7A1* mRNA in LV-RTM-S6m transduced RDEB cell pool and single cell clone C47. LV-RTM-woBD transduced cells served as negative control. (**B**) Sequence analysis of trans-spliced *COL7A1* mRNA shows the correct exon 64/65 junction as well as the amplified silent mutations. (**C**) SqRT-PCR analysis showed that 2.113% of *COL7A1* mRNA in C47 was correctly *trans*-spliced. Mean of four individual experiments and error bars (SEM). ***P-value < 0.001.

GFP sequence of the integrated vector, expecting a band of >6149 bp in size, depending on the following, unknown Asp718 restriction site within the genome, where integration occurred (Supplementary Figure S3B). For C47, there is only one band of approximately 7 kb, suggesting single copy integration, subscribing the result from PCR analysis. For the polyclonal LV-RTM-S6m cell pool, we expected several bands larger than 6 kb. The reason why there is apparently only one (slightly higher than the band in C47) is probably that very high molecular weight bands cannot be discriminated in a Southern blot as discrete bands (Supplementary Figure S3C). We detected an additional band at ∼3 kb in the transduced cell pool, which potentially correspond to additional shortened RTM products generated during the viral transduction procedure. The presence of rearranged copies of the vector might be related to truncated type VII collagen protein expression at 150 kDa detected in Western blot analysis (Supplementary Figure S4).

The integration locus was detected via linear amplification–mediated (LAM) PCR in an intergenic region on chromosome 19 in C47 ranging from nt position 50 427 188 to nt position 50 427 249. The nearest gene to the proviral integration site in C47, mapped on the human genome, is activation transcription factor 5 (*ATF5*) whose transcription start site (TSS) is 4786 nt upstream from the viral integration site (Supplementary Figure S3A). RT-PCR analysis performed on normal, untransduced and transduced C47 keratinocyte cultures showed no change in the expression of *ATF5*, indicating no dysregulation due to the proviral integration (Supplementary Figure S3D).

Skin grafts of C47 showed long-term correction of the RDEB phenotype in a mouse model

Skin equivalents generated from LV-RTM-S6m corrected RDEB keratinocytes C47 were grafted onto the back of immunodeficient mice (21–23). We analyzed the grafts 4 weeks after transplantation, revealing corrected type VII collagen expression at the BMZ, which showed the functionality of the approach (data not shown). In order to evaluate the continuity of phenotypic correction over a longer period of time, we analyzed skin grafts 12 weeks after transplantation, showing via histological analysis differentiation and stratification as expected for regenerated human skin derived from an immortalized cell line (Figure 6A–C). H&E staining of murine tissue highlights the differences of

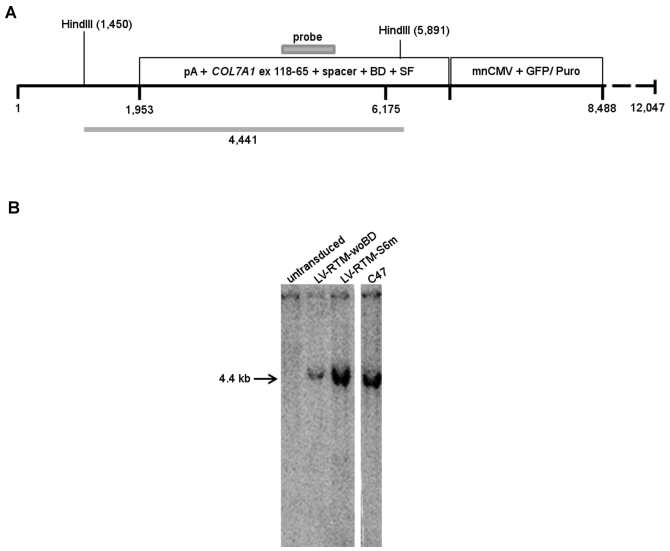

Figure 5. Full-length integration of the provirus into the C47 genome. (**A**) Full-length RTM integration was detected by Southern Blot analysis using HindIII, flanking the RTM, and a 327 bp probe spanning from *COL7A1* exon 70 to parts of the spacer sequence of LV-RTM-S6m, expecting a predicted band size of 4441 bp upon RTM integration. (**B**) Southern blot analysis showed full-length RTM integration in LV-RTM-S6m and LV-RTM-woBD transduced keratinocyte pool, as well as in single cell clone C47 by detecting a band at 4.4 kb.

grafted human tissue and murine skin, showing no skin appendages, such as hair follicles (Figure 6D). Immunofluorescence staining using an antibody against human type VII collagen, showed strong labelling along the BMZ in skin equivalents (SE) derived from C47 (Figure 6G), and from normal human keratinocytes (Figure 6F), weakly visible in SE derived from untransduced keratinocytes (Figure 6E). Localization of human type VII collagen using a species specific antibody was restricted to the basement membrane, with no expression in the suprabasal cell layers. We included a murine tissue section, showing no specific signal at the BMZ which confirms the human origin of the analysed skin grafts (Figure 6h). Involucrin, specifically expressed in the upper epidermal layers, further confirmed the human origin of harvested SE by detecting a green fluorescence signal exclusively in the upper epidermal layers in all grafted SE (Supplementary Figure S5A–C). We included murine tissue as negative control, detecting an unspecific fluorescent signal in all epidermal layers and the dermis, due to the presence of host IgGs reacting with the anti mouse secondary antibody (Supplementary Figure S5D).

DISCUSSION

We have developed an *ex vivo* therapy approach applying an optimized 3′ RTM (LV-RTM-S6m) in a xenograft mouse model, which resulted in long-term type VII collagen expression in skin derived from *trans*-splicing corrected patient keratinocytes.

To ensure long-term expression of the transgene for gene therapeutic approaches, stable genome integration is needed, using gammaretro- or lentiviral vectors. Contemporaneously, the risk of proto-oncogene activation as a consequence of vector integration is a precarious topic, since serious implications including the development of myeloproliferative diseases and leukemias are possible (28,29). Although *ex vivo* gene therapy, using a replication-defective Moloney-derived retroviral LTR-driven vector was successful to treat the rare immune deficiency disorder X-SCID, some patients developed leukemia as a severe adverse event. Insertional analysis from treated patients demonstrated several integration sites enriched near transcription start sites (30,31). Therefore, the possibility of isolating single cell clones in the course of an *ex vivo* therapy for the skin, and determination of amount and location of the proviral integration in the cell's genome prior to transplantation, reduces the risk of severe adverse events (32,33). In this study, even an integration close to *ATF5* gene did not lead to vector associated deregulation. A residual risk remains, but since the skin is an easy accessible organ, malignant transformation of cells in gene-corrected transplanted skin are much easier to handle compared to gene therapy approaches in the blood system, where the corrected cells are injected into the bloodstream. Therefore, the potential occurrence of tumor formation can be recognized at early stages and corresponding measures like surgical removal can be initiated.

A successful application of a cutaneous *ex vivo* gene therapy has already been described for two patients suffering from the junctional form of EB caused by mutations within the *LAMB3* gene. In these studies, epidermal stem cells were isolated from the patient's skin, corrected using a gammaretroviral vector containing a wild-type copy of the *LAMB3* cDNA, expanded to epidermal grafts and retransplanted onto the patients' wounds. In both patients, laminin-332 expression within the basal membrane zone was maintained through the entire follow-up period of 8 years and 16 months, respectively with no evidence of blistering, inflammation, tumor formation or immune response in the grafted area (34–37). These studies underscore the safety of using standard viral vectors in combination with an *ex vivo* gene therapy applied on the skin. However, in our study we put even more emphasis on a safe viral-mediated *ex vivo* therapy by focusing on the use of a safety-optimized lentiviral SIN vector backbone. A deletion in the 3′ LTR abolishes the activity of the viral enhancer-promoter sequence leading to a reduced risk of insertional mutagenesis and oncogene activation is reduced compared to vectors with active LTRs (38–40). This architecture was successfully used in the setting of clinical trials for immunodeficiencies (41). Compared to gammaretroviral vectors, lentiviral vectors allow infection of both, dividing and non-dividing cells, ideally applicable for keratinocytes, providing a low cell division rate (42). Indeed, the use of a SIN lentiviral vector represents a safer way to integrate DNA into the genome (43), but undesired effects caused by insertional modified regulation of gene expression at the transcriptional and post-transcriptional level are still possible. During viral transduction the number of integrations into the cell's genome varies from cell to cell and is difficult to control. In this study, we have isolated an ideal single cell clone, carrying one proviral copy, thereby reducing the risk of genomic modifications to a minimum, while providing sufficient RTM-S6m expression to generate an adequate

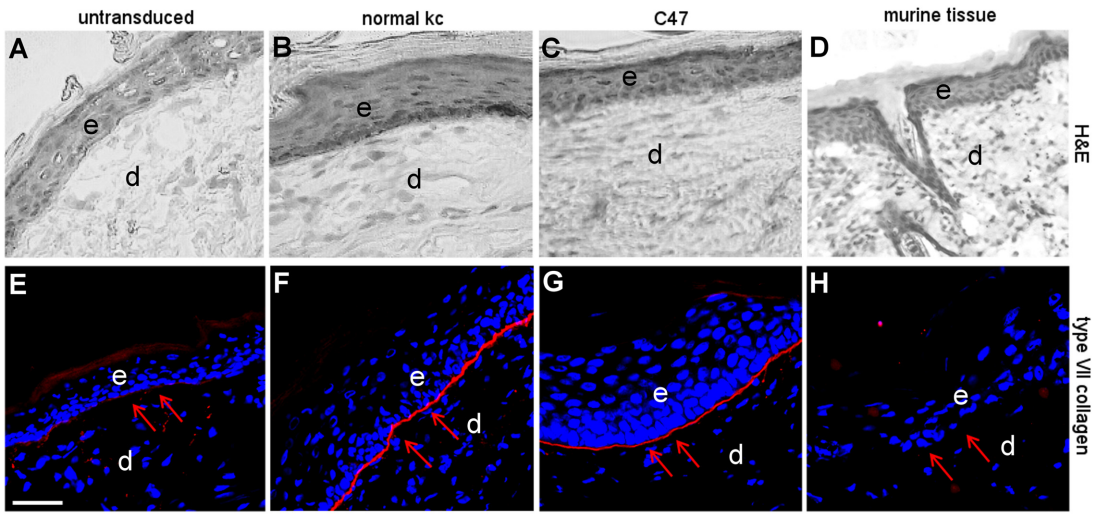

Figure 6. Grafting of skin equivalents derived from C47 revealed long-term correction of the RDEB phenotype. (**A**–**D**) H&E staining of 12 weeks old skin grafts derived from C47 (C), normal keratinocytes (B), and untransduced keratinocytes (A) showed normal differentiation into human skin. As a control we included a murine tissue sample (D). **(E**–**H)** Immunofluorescence staining of type VII collagen in 12 weeks old skin grafts derived from C47 (G) showed protein expression at the BMZ (red) at comparable levels as detected in grafts from normal human keratinocytes (F). Grafts expanded from untransduced RDEB keratinocytes (E) showed only weak type VII collagen expression at the BMZ. As negative control, we included murine wild-type tissue (H). The cell nuclei were stained with DAPI (blue). e = epidermis; d = dermis. C7 = type VII collagen. SB = 50 μm.

level of RNA *trans*-splicing-mediated repair efficiency to correct the RDEB phenotype.

Our established RTM can correct ∼40% of all DEB causing mutations, including several hot spot mutations (15,16). Compared to genome editing technologies such as CRISPR/Cas9 and TALEN enabling mutation-specific correction of donor cells at genomic level, the use of this RTM can be applied to a larger number of patients, avoiding costly production of patient-tailored molecules. Further, it has been shown that viral transduction of the 8.9 kb full-length *COL7A1* cDNA into RDEB keratinocytes can lead to shortened *COL7A1* cDNA fragment integration into the cell's genome, probably generated during the reverse transcription process, evoked by the huge *COL7A1* transcript size including a high number of repetitive sequences (44). The shorter *COL7A1* cDNA transgene (3.6 kb), expressed from LV-RTM-S6m, reduces the risk of DNA rearrangement during viral packaging and thus the risk of shortened protein translation. We further omitted the problem of unwanted rearranged *COL7A1* transcripts by RTM optimization. Western blot analysis revealed no shortened protein fragments derived from the lenti-transcription process, unspecific RTM splicing or direct RTM expression in the single cell clone C47. Instead, the expression of a full-length 290 kDa protein indicated that correct *trans*-splicing occurred through a correctly integrated LV-RTM-S6m. Additionally, Southern blot analysis confirmed full-length RTM-S6m integration and the absence of rearranged, size-reduced *COL7A1* DNA fragments in C47. These results demonstrate the increased safety of the RNA *trans*-splicing technology for *COL7A1* targeting approaches, compared to full-length cDNA replacement, avoiding the unknown effects, which truncated protein expression could exhibit in a clinical setting. However, generation of truncated protein versions during the lentiviral transduction still remains challenging, as demonstrated by protein analysis of the LV-RTM-S6m transduced cell pool. Therefore, codon-optimization as previously described by Georgiadis *et al.* exhibits a promising option. Elimination of almost all repetitive sequences within *COL7A1* lead to expression of abnormally sized protein in only 3 of 49 single cell clonal population (45).

Although we have put much effort into the optimization of the RTM design using the knowledge from previous studies (24,46), low efficiencies have still constituted an obstacle in the process of bringing the RNA *trans*-splicing technology into the clinic. In general, the endogenous *cis*-splicing reaction in an RTM transduced cell pool is strongly favored compared to the competitive *trans*-splicing event. Even so, the detection of *trans*-spliced mRNA and type VII collagen expression is possible, the quantification of the corrected *COL7A1* mRNA level via sqRT-PCR remains difficult. Further, the amount of corrected type VII collagen for a clinical application would be too low if the transduced cell pool, showing a very heterogenous type VII collagen expression pattern, was used for the generation of transplantable skin sheets. Therefore, the isolation of a single cell clone, producing high levels of repaired type VII collagen, is essentially required. Put in perspective to other therapy approaches, like the TALEN technology as a genome editing approach, the need of highly efficient single cell clones for clinical applications has already been reported (47).

With regard to a clinical *ex vivo* approach in patients, suffering from RDEB, Fritsch *et al* developed a *Col7a1* hypomorphic mouse model, which expresses only ∼10% of type VII collagen and is viable up to one year, indicating that low levels of protein expression can already improve the severe phenotype (48). We showed that the accumulation of translated proteins derived from only ∼2% of corrected *COL7A1* mRNA is sufficient for ∼ 53% type VII collagen

expression and correction of the RDEB phenotype. We hypothesize that mutated *cis*-spliced mRNA is degraded prior to translation, allowing the small amount of *trans*-spliced mRNA to compensate for the previous lack of type VII collagen expression. Additionally, the fact that the *trans*-spliced *COL7A1* mRNA lacks of the 3′ UTR might increase its stability, which could lead to favored protein translation of the corrected mRNA over the *cis*-spliced mRNA including the 3′ UTR. This might be due to the binding of microRNAs to the 3′ UTR in the diseased RDEB keratinocytes, which either can lead to degradation of the mRNA or inhibition of the protein translation (49).

Upon grafting of skin equivalents derived from *trans*-splicing corrected immortalized keratinocytes, we detected normal type VII collagen expression levels at the BMZ for at least 12 weeks. The stable integration into the genome of the cell line provides permanent transgene expression and thus permanent protein correction. However, in the course of an *ex vivo* therapy in patients, the crucial point is to target stem cells to ensure a long term graft maintenance.

In summary, we have improved the previously described RTM-S6 (14) in terms of safety in order to correct RDEB keratinocytes carrying a homozygous mutation in exon 80 (c.6527dupC) *in vitro* and *ex vivo.* This RTM-S6m can be used to correct mutations located in the 3′ part of the *COL7A1* gene downstream to exon 65, encompassing ∼40% of all known DEB causing mutations (15,16). Regarding the design, packaging and delivery of LV-RTM-S6m, we managed to establish an *ex vivo* protocol fulfilling necessary safety criteria and effective correction of the RDEB phenotype and can thus be applied in a clinical setting.

SUPPLEMENTARY DATA

Supplementary Data are available at NAR Online.

ACKNOWLEDGEMENTS

We thank Dr. Andrea Zurl from University Clinic of Ophthalmology and Optometry in Salzburg, Austria, for offering microscopy analysis and Dr. Alexander Nyström from the Department of Dermatology, University Medical Center, Freiburg, Germany, for providing the type VII collagen specific antibody.

FUNDING

Anniversary Fund of the Oesterreichische Nationalbank [OeNB Project No. 15941 to D.S., G.B.]; Austrian Science Fund (FWF) [E-RARE2; Project I1175-B13]; DEBRA Austria and DFG [SFB738, REBIRTH Cluster of Excellence]; Spanish ISCIII [PI14/00931 to R.M., B.D., F.L.]; MINECO [SAF2013-43475-R to M.G., R.M.]. Funding for open access charge: Austrian Science Fund (FWF) [E-RARE2; Project I1175-B13].

Conflict of interest statement. Johann W. Bauer is inventor on US (US8735366) and European (EP2320952) patent 'Improved pre-mRNA trans-splicing molecules (RTM) and their uses'.

REFERENCES

1. Fine,J.D. and Hintner,H. (2009) *Life with Epidermolysis Bullosa (EB): Etiology, Diagnosis, Multicisciplinary Care and Therapy*.
2. Fine,J.D. (2010) Inherited epidermolysis bullosa. *Orphanet. J. Rare Dis.*, **5**, 12.
3. Soro,L., Bartus,C. and Purcell,S. (2015) Recessive dystrophic epidermolysis bullosa: a review of disease pathogenesis and update on future therapies. *J. Clin. Aesthet. Dermatol.*, **8**, 41–46.
4. Weber,F., Bauer,J.W., Sepp,N., Hogler,W., Salmhofer,W., Hintner,H. and Fritsch,P. (2001) Squamous cell carcinoma in junctional and dystrophic epidermolysis bullosa. *Acta Derm. Venereol.*, **81**, 189–192.
5. Siprashvili,Z., Nguyen,N.T., Gorell,E.S., Loutit,K., Khuu,P., Furukawa,L.K., Lorenz,H.P., Leung,T.H., Keene,D.R., Rieger,K.E. *et al.* (2016) Safety and wound outcomes following genetically corrected autologous epidermal grafts in patients with recessive dystrophic Epidermolysis bullosa. *JAMA*, **316**, 1808–1817.
6. Kumar,M., Keller,B., Makalou,N. and Sutton,R.E. (2001) Systematic determination of the packaging limit of lentiviral vectors. *Hum. Gene Ther.*, **12**, 1893–1905.
7. Wally,V., Murauer,E.M. and Bauer,J.W. (2012) Spliceosome-mediated trans-splicing: the therapeutic cut and paste. *J. Invest. Dermatol.*, **132**, 1959–1966.
8. Koller,U., Wally,V., Bauer,J.W. and Murauer,E.M. (2014) Considerations for a successful RNA trans-splicing repair of genetic disorders. *Mol. Ther. Nucleic Acids*, **3**, e157.
9. Coady,T.H. and Lorson,C.L. (2010) Trans-splicing-mediated improvement in a severe mouse model of spinal muscular atrophy. *J. Neurosci.*, **30**, 126–130.
10. Rindt,H., Yen,P.F., Thebeau,C.N., Peterson,T.S., Weisman,G.A. and Lorson,C.L. (2012) Replacement of huntingtin exon 1 by trans-splicing. *Cell Mol. Life Sci.*, **69**, 4191–4204.
11. Avale,M.E., Rodriguez-Martin,T. and Gallo,J.M. (2013) Trans-splicing correction of tau isoform imbalance in a mouse model of tau mis-splicing. *Hum. Mol. Genet.*, **22**, 2603–2611.
12. Peking,P., Koller,U., Hainzl,S., Kitzmueller,S., Kocher,T., Mayr,E., Nystrom,A., Lener,T., Reichelt,J. and Bauer,J.W. (2016) A gene gun-mediated non-viral RNA trans-splicing strategy for Col7a1 repair. *Mol Ther Nucleic Acids*, **5**, e287.
13. Wally,V., Brunner,M., Lettner,T., Wagner,M., Koller,U., Trost,A., Murauer,E.M., Hainzl,S., Hintner,H. and Bauer,J.W. (2010) K14 mRNA reprogramming for dominant epidermolysis bullosa simplex. *Hum. Mol. Genet.*, **19**, 4715–4725.
14. Murauer,E.M., Gache,Y., Gratz,I.K., Klausegger,A., Muss,W., Gruber,C., Meneguzzi,G., Hintner,H. and Bauer,J.W. (2011) Functional correction of type VII collagen expression in dystrophic epidermolysis bullosa. *J. Invest. Dermatol.*, **131**, 74–83.
15. Wertheim-Tysarowska,K., Sobczynska-Tomaszewska,A., Kowalewski,C., Skronski,M., Swieckowski,G., Kutkowska-Kazmierczak,A., Wozniak,K. and Bal,J. (2012) The COL7A1 mutation database. *Hum. Mutat.*, **33**, 327–331.
16. van den Akker,P.C., Jonkman,M.F., Rengaw,T., Bruckner-Tuderman,L., Has,C., Bauer,J.W., Klausegger,A., Zambruno,G., Castiglia,D., Mellerio,J.E. *et al.* (2011) The international dystrophic epidermolysis bullosa patient registry: an online database of dystrophic epidermolysis bullosa patients and their COL7A1 mutations. *Hum. Mutat.*, **32**, 1100–1107.
17. Maetzig,T., Galla,M., Brugman,M.H., Loew,R., Baum,C. and Schambach,A. (2010) Mechanisms controlling titer and expression of bidirectional lentiviral and gammaretroviral vectors. *Gene Ther.*, **17**, 400–411.
18. Chamorro,C., Almarza,D., Duarte,B., Llames,S.G., Murillas,R., Garcia,M., Cigudosa,J.C., Espinosa-Hevia,L., Escamez,M.J., Mencia,A. *et al.* (2013) Keratinocyte cell lines derived from severe generalized recessive epidermolysis bullosa patients carrying a highly recurrent COL7A1 homozygous mutation: models to assess cell and gene therapies in vitro and in vivo. *Exp. Dermatol.*, **22**, 601–603.
19. Rheinwald,J.G. and Green,H. (1974) Growth of cultured mammalian cells on secondary glucose sources. *Cell*, **2**, 287–293.
20. Koller,U., Hainzl,S., Kocher,T., Huttner,C., Klausegger,A., Gruber,C., Mayr,E., Wally,V., Bauer,J.W. and Murauer,E.M. (2015) Trans-splicing improvement by the combined application of antisense strategies. *Int. J. Mol. Sci.*, **16**, 1179–1191.

21. Del Rio,M., Larcher,F., Serrano,F., Meana,A., Munoz,M., Garcia,M., Munoz,E., Martin,C., Bernad,A. and Jorcano,J.L. (2002) A preclinical model for the analysis of genetically modified human skin in vivo. *Hum. Gene Ther.*, **13**, 959–968.
22. Garcia,M., Llames,S., Garcia,E., Meana,A., Cuadrado,N., Recasens,M., Puig,S., Nagore,E., Illera,N., Jorcano,J.L. *et al.* (2010) In vivo assessment of acute UVB responses in normal and Xeroderma Pigmentosum (XP-C) skin-humanized mouse models. *Am. J. Pathol.*, **177**, 865–872.
23. Garcia,M., Larcher,F., Hickerson,R.P., Baselga,E., Leachman,S.A., Kaspar,R.L. and Del Rio,M. (2011) Development of skin-humanized mouse models of pachyonychia congenita. *J. Invest. Dermatol.*, **131**, 1053–1060.
24. Murauer,E.M., Koller,U., Hainzl,S., Wally,V. and Bauer,J.W. (2013) A reporter-based screen to identify potent 3′ trans-splicing molecules for endogenous RNA repair. *Hum. Gene Ther. Methods*, **24**, 19–27.
25. Lapiere,J.C., Chen,J.D., Iwasaki,T., Hu,L., Uitto,J. and Woodley,D.T. (1994) Type VII collagen specifically binds fibronectin via a unique subdomain within the collagenous triple helix. *J. Invest. Dermatol.*, **103**, 637–641.
26. Brittingham,R., Uitto,J. and Fertala,A. (2006) High-affinity binding of the NC1 domain of collagen VII to laminin 5 and collagen IV. *Biochem. Biophys. Res. Commun.*, **343**, 692–699.
27. Chen,M., Marinkovich,M.P., Veis,A., Cai,X., Rao,C.N., O'Toole,E.A. and Woodley,D.T. (1997) Interactions of the amino-terminal noncollagenous (NC1) domain of type VII collagen with extracellular matrix components. A potential role in epidermal-dermal adherence in human skin. *J. Biol. Chem.*, **272**, 14516–14522.
28. Stein,S., Scholz,S., Schwable,J., Sadat,M.A., Modlich,U., Schultze-Strasser,S., Diaz,M., Chen-Wichmann,L., Muller-Kuller,U., Brendel,C. *et al.* (2013) From bench to bedside: preclinical evaluation of a self-inactivating gammaretroviral vector for the gene therapy of X-linked chronic granulomatous disease. *Hum. Gene Ther. Clin. Dev.*, **24**, 86–98.
29. Cavazzana-Calvo,M., Fischer,A., Hacein-Bey-Abina,S. and Aiuti,A. (2012) Gene therapy for primary immunodeficiencies: Part 1. *Curr. Opin. Immunol.*, **24**, 580–584.
30. Hacein-Bey-Abina,S., Garrigue,A., Wang,G.P., Soulier,J., Lim,A., Morillon,E., Clappier,E., Caccavelli,L., Delabesse,E., Beldjord,K. *et al.* (2008) Insertional oncogenesis in 4 patients after retrovirus-mediated gene therapy of SCID-X1. *J. Clin. Invest.*, **118**, 3132–3142.
31. Hacein-Bey-Abina,S., von Kalle,C., Schmidt,M., Le Deist,F., Wulffraat,N., McIntyre,E., Radford,I., Villeval,J.L., Fraser,C.C., Cavazzana-Calvo,M. *et al.* (2003) A serious adverse event after successful gene therapy for X-linked severe combined immunodeficiency. *N. Engl. J. Med.*, **348**, 255–256.
32. Larcher,F., Dellambra,E., Rico,L., Bondanza,S., Murillas,R., Cattoglio,C., Mavilio,F., Jorcano,J.L., Zambruno,G. and Del Rio,M. (2007) Long-term engraftment of single genetically modified human epidermal holoclones enables safety pre-assessment of cutaneous gene therapy. *Mol. Ther.*, **15**, 1670–1676.
33. Droz-Georget Lathion,S., Rochat,A., Knott,G., Recchia,A., Martinet,D., Benmohammed,S., Grasset,N., Zaffalon,A., Besuchet Schmutz,N., Savioz-Dayer,E. *et al.* (2015) A single epidermal stem cell strategy for safe ex vivo gene therapy. *EMBO Mol. Med.*, **7**, 380–393.
34. Mavilio,F., Pellegrini,G., Ferrari,S., Di Nunzio,F., Di Iorio,E., Recchia,A., Maruggi,G., Ferrari,G., Provasi,E., Bonini,C. *et al.* (2006) Correction of junctional epidermolysis bullosa by transplantation of genetically modified epidermal stem cells. *Nat. Med.*, **12**, 1397–1402.
35. Murauer,E.M., Koller,U., Pellegrini,G., De Luca,M. and Bauer,J.W. (2015) Advances in gene/cell therapy in Epidermolysis bullosa. *Keio J. Med.*, **64**, 21–25.
36. De Rosa,L., Carulli,S., Cocchiarella,F., Quaglino,D., Enzo,E., Franchini,E., Giannetti,A., De Santis,G., Recchia,A., Pellegrini,G. *et al.* (2014) Long-term stability and safety of transgenic cultured epidermal stem cells in gene therapy of junctional epidermolysis bullosa. *Stem Cell Rep.*, **2**, 1–8.
37. Bauer,J.W., Koller,J., Murauer,E.M., De Rosa,L., Enzo,E., Carulli,S., Bondanza,S., Recchia,A., Muss,W., Diem,A. *et al.* (2017) Closure of a large chronic wound through transplantation of gene-corrected epidermal stem cells. *J. Invest. Dermatol.*, **137**, 778–781.
38. Schambach,A., Bohne,J., Chandra,S., Will,E., Margison,G.P., Williams,D.A. and Baum,C. (2006) Equal potency of gammaretroviral and lentiviral SIN vectors for expression of O6-methylguanine-DNA methyltransferase in hematopoietic cells. *Mol. Ther.*, **13**, 391–400.
39. Zufferey,R., Dull,T., Mandel,R.J., Bukovsky,A., Quiroz,D., Naldini,L. and Trono,D. (1998) Self-inactivating lentivirus vector for safe and efficient in vivo gene delivery. *J. Virol.*, **72**, 9873–9880.
40. Cesana,D., Sgualdino,J., Rudilosso,L., Merella,S., Naldini,L. and Montini,E. (2012) Whole transcriptome characterization of aberrant splicing events induced by lentiviral vector integrations. *J. Clin. Invest.*, **122**, 1667–1676.
41. Biffi,A., Montini,E., Lorioli,L., Cesani,M., Fumagalli,F., Plati,T., Baldoli,C., Martino,S., Calabria,A., Canale,S. *et al.* (2013) Lentiviral hematopoietic stem cell gene therapy benefits metachromatic leukodystrophy. *Science*, **341**, 1233158.
42. Kuhn,U., Terunuma,A., Pfutzner,W., Foster,R.A. and Vogel,J.C. (2002) In vivo assessment of gene delivery to keratinocytes by lentiviral vectors. *J. Virol.*, **76**, 1496–1504.
43. Cavazza,A., Cocchiarella,F., Bartholomae,C., Schmidt,M., Pincelli,C., Larcher,F. and Mavilio,F. (2013) Self-inactivating MLV vectors have a reduced genotoxic profile in human epidermal keratinocytes. *Gene Ther.*, **20**, 949–957.
44. Titeux,M., Pendaries,V., Zanta-Boussif,M.A., Decha,A., Pironon,N., Tonasso,L., Mejia,J.E., Brice,A., Danos,O. and Hovnanian,A. (2010) SIN retroviral vectors expressing COL7A1 under human promoters for ex vivo gene therapy of recessive dystrophic epidermolysis bullosa. *Mol. Ther.*, **18**, 1509–1518.
45. Georgiadis,C., Syed,F., Petrova,A., Abdul-Wahab,A., Lwin,S.M., Farzaneh,F., Chan,L., Ghani,S., Fleck,R.A., Glover,L. *et al.* (2016) Lentiviral engineered fibroblasts expressing codon-optimized COL7A1 restore anchoring fibrils in RDEB. *J. Invest. Dermatol.*, **136**, 284–292.
46. Wally,V., Koller,U. and Bauer,J.W. (2011) High-throughput screening for highly functional RNA-trans-splicing molecules: correction of plectin in Epidermolysis bullosa simplex: human genetic diseases. *InTech*, doi:10.5772/24149.
47. Osborn,M.J., Starker,C.G., McElroy,A.N., Webber,B.R., Riddle,M.J., Xia,L., DeFeo,A.P., Gabriel,R., Schmidt,M., von Kalle,C. *et al.* (2013) TALEN-based gene correction for epidermolysis bullosa. *Mol. Ther.*, **21**, 1151–1159.
48. Fritsch,A., Loeckermann,S., Kern,J.S., Braun,A., Bosl,M.R., Bley,T.A., Schumann,H., von Elverfeldt,D., Paul,D., Erlacher,M. *et al.* (2008) A hypomorphic mouse model of dystrophic epidermolysis bullosa reveals mechanisms of disease and response to fibroblast therapy. *J. Clin. Invest.*, **118**, 1669–1679.
49. Cannell,I.G., Kong,Y.W. and Bushell,M. (2008) How do microRNAs regulate gene expression? *Biochem. Soc. Trans.*, **36**, 1224–1231.